Original Article

Osteogenic potential of poly(ethylene glycol)-amorphous calcium phosphate composites on human mesenchymal stem cells

Journal of Tissue Engineering
Volume 11: 1–13

DOI: 10.1177/2041731420926840
journals.sagepub.com/home/tej
SAGE

Aman S Chahal[1*], Manuel Schweikle[1*], Aina-Mari Lian[2], Janne E Reseland[1], Håvard J Haugen[1] and Hanna Tiainen[1]

Abstract

Synthetic hydrogel-amorphous calcium phosphate composites are promising candidates to substitute biologically sourced scaffolds for bone repair. While the hydrogel matrix serves as a template for stem cell colonisation, amorphous calcium phosphate s provide mechanical integrity with the potential to stimulate osteogenic differentiation. Here, we utilise composites of poly(ethylene glycol)-based hydrogels and differently stabilised amorphous calcium phosphate to investigate potential effects on attachment and osteogenic differentiation of human mesenchymal stem cells. We found that functionalisation with integrin binding motifs in the form of RGD tripeptide was necessary to allow adhesion of large numbers of cells in spread morphology. Slow dissolution of amorphous calcium phosphate mineral in the scaffolds over at least 21 days was observed, resulting in the release of calcium and zinc ions into the cell culture medium. While we qualitatively observed an increasingly mineralised extracellular matrix along with calcium deposition in the presence of amorphous calcium phosphate-loaded scaffolds, we did not observe significant changes in the expression of selected osteogenic markers.

Keywords

Hydrogel, PEG, human mesenchymal stem cells, cell differentiation, calcium phosphate, tissue engineering, citrate, zinc, ACP

Date received: 14 January 2020; accepted: 22 April 2020

Introduction

Grafting of non-healing bone defects is an important medical therapy with 2.2 million yearly procedures worldwide.[1] Currently, the majority of transplants rely on autologous, allogeneic or xenogeneic sources.[1,2] This entails potentially painful, lengthy and costly procedures, bearing the risk of transferring diseases.[2–6] Easily applicable alloplastic scaffolds can overcome these limitations: they are readily available, safe, and can drastically cut down treatment times and costs.[1,6]

Current alloplastic scaffold designs commonly employ crystalline calcium phosphates (CaP) in a polymeric matrix in an attempt to mimic the composite structure of biological bone tissue.[6,7] Conventional synthetic scaffolds, however, do not reach the regenerative performance of naturally derived bone grafts.[1] The synthetic bone graft substitutes are lacking the osteoinductive properties of biological bone grafts[6] and highly crystalline CaPs are insufficiently

[1]Department of Biomaterials, Institute of Clinical Dentistry, University of Oslo, Oslo, Norway
[2]Oral Research Laboratory, Institute of Clinical Dentistry, University of Oslo, Oslo, Norway

* A.S.C. and M.S. contributed equally to this study and should be considered first author.

Corresponding author:
Hanna Tiainen, Department of Biomaterials, Institute of Clinical Dentistry, University of Oslo, Geitmyrsveien 69-71, 0455 Oslo, Norway.
Email: hanna.tiainen@odont.uio.no

Table 1. Overview of the scaffold compositions.

Designation	Polymer (wt. %)	cRGD (mM)	Ammonium phosphate (mM)	Calcium nitrate (mM)	Zinc nitrate (mM)	Ammonium citrate (mM)
N	5	–	–	–	–	–
NR	5	2.5	–	–	–	–
C	5	–	200	400	–	50
CR	5	2.5	200	400	–	50
Z	5	–	200	360	40	–
ZR	5	2.5	200	360	40	–

resorbed and remodelled into the poorly crystalline, calcium-deficient hydroxyapatite (HA), which constitutes the majority of natural bone mineral.[8] We suggest that instead of mimicking mature bone, synthetic bone scaffolds should be designed as a temporary matrix that stimulates bone formation and can easily be replaced with newly formed bone tissue by cellular activity.

We previously mineralised enzymatically degradable synthetic poly(ethylene glycol) (PEG)-based hydrogel matrices that have been shown to be highly suitable for bone repair applications[9,10] with amorphous calcium phosphate (ACP) of variable stability.[11] In contrast to the highly crystalline CaP phases that are commonly studied in bone graft substitutes, composites in which 10% of the calcium ions were substituted with zinc featured stable ACP, while ACP in citrate-stabilised composites transformed via octacalcium phosphate into HA within days. Both composites released calcium or calcium and zinc ions in a two-stage manner: a high initial burst release followed by a sustained release over several weeks. However, the impact of soluble minerals released from these systems on human cells has not yet been elucidated.

Experimental evidence indicates that cells perceive the presence of extracellular, soluble minerals as paracrine signals capable of triggering proliferation and differentiation pathways.[12] Particularly, soluble zinc has been demonstrated to induce osteogenic differentiation and bone formation,[13,14] while calcium-sensing receptors (CaSRs) and calcium/calmodulin-dependent protein kinase 2 (CaMK) have been identified as drivers in the differentiation process of cells.[15–17] Previous studies show that zinc not only enhanced alkaline phosphatase (ALP) activity in bone marrow stromal cells,[18] but also had an inhibitory effect on the resorbing activity of osteoclasts.[19] Furthermore, long-term *in vivo* studies have proven zinc releasing calcium phosphates to be stimulatory in bone formation.[20] We hypothesise that synthetic hydrogel scaffolds mineralised with stabilised ACP outperform conventional synthetic bone graft substitutes as a sustained release of calcium and zinc ions from the former drives osteogenic differentiation of stem cells in adjacent tissues.

The aim of the present study is to investigate the potential of soluble factors released from composite scaffolds to stimulate osteogenic differentiation of primary human mesenchymal stem cells (hMSCs). Therefore, we characterised the physical properties of the composites and measured the cation release under cell culture conditions. Cell stimulation was assessed in terms of attachment, cytotoxicity, metabolic activity, gene expression, protein and cytokine production, and matrix formation.

Material and methods

Scaffold fabrication

Plain or mineralised hydrogel scaffolds were produced as previously described by mixing two precursor solutions.[11] Component A contained maleimide-functionalised PEG macromers (8-armed macromers, 40 kDa, JenKem Technologies USA, Plano, TX) in an ammonium phosphate solution at pH 5.5. Component B contained an amount of enzymatically cleavable end-linking peptide (AcGCRDVPMSMRGGDRCGNH$_2$,[21] GenScript, Piscataway, NJ) stoichiometrically matching the number of free maleimide groups in component A and calcium nitrate. Final samples contained 5 wt. % polymer, 200 mM phosphate and 400 mM calcium. Citrate stabilised scaffolds (C) contained additionally 50 mM ammonium citrate (added to component A). In zinc-stabilised scaffolds (Z), 10 mol. % of the calcium in component B were substituted with zinc. Non-mineralised scaffolds (N) contained no calcium in component B. In some groups (suffix R), cell binding sites were incorporated attaching 2.5 mM of a cyclic RGD (cRGD) motif (Cyclo(RGD(dF)C), AnaSpec, Fremont, CA) to the polymer prior to gelation as previously reported.[22] All base reagents were purchased from Sigma Aldrich (Oslo, Norway). An overview of the scaffold compositions is provided in Table 1.

Mechanical scaffold characterisation

Volume swelling ratios were determined on disc-shaped scaffolds using the buoyancy principle. Sample volumes were determined after 10 min of curing and after distinct time intervals of swelling in MSC basal medium (MSCBM™, PT3238, Lonza, Basel, Switzerland) at 37°C. Mechanical properties of swollen scaffolds were assessed by oscillatory shear measurements as previously described.[23] Large scaffold discs (⌀ 25 mm, t ~1.6 mm) were loaded on

a plate-plate geometry of a rheometer (PP25 on an MCR 301, Anton Paar, Graz, Austria) and pre-compressed with a normal force of 0.5 N to prevent slip. Oscillatory frequency sweeps were performed at 0.1% and 1% strain. Amplitude sweeps performed at 1 Hz confirmed that the measurements were performed within the linear viscoelastic regime and samples were fully recovered before starting a new measurement. All measurements were performed at 37°C. In all material characterisation experiments, cRGD-functionalisation was mimicked using *N*-acetyl-cysteine in place of cRGD. All material characterisation was performed on three independent replicates. Media was replaced every 72 h for all cell experiments.

General cell culture

All cell studies were performed using bone-marrow-derived hMSCs purchased from Lonza (lot 0000451491, tissue acquisition 28386, Lonza, Basel, Switzerland). Cells were cultured (passage ⩽ 5) at 37°C in a humidified incubator at 5% CO_2. Undifferentiated cells were expanded in MSCBM™ supplemented with MSCGM™ hMSC SingleQuots (PT3238 and PT4105, Lonza, Basel, Switzerland). At 70% confluence, cells were trypsinised for seeding. Medium used during cell attachment and exposure experiments was supplemented with dexamethasone (10 nM), ascorbic acid (0.28 mM) and beta-glycerol phosphate (10 μM). Supplements were always added freshly before medium changes throughout the experiments.

Cell attachment

For cell attachment studies, 3.0 x 10^3 hMSCs in 30 μL of media were seeded directly on the surfaces of non-mineralised and mineralised hydrogel scaffolds with and without cRGD functionalisation (discs, ⌀ ~5 mm, t ~1 mm). Cells seeded on scaffolds were allowed to attach for 1.5 h at 37°C in a humidified incubator before adding 1 mL of medium. For confocal imaging, hMSCs were fixed after 48 h of culture by adding 4% paraformaldehyde (PFA) solution in a 1:1 ratio directly to the medium for 10 min. Subsequently, medium and PFA was discarded and replaced with pure 4% PFA solution for 20 min. Cells were then washed twice with phosphate buffered saline (PBS) and permeabilised using 0.1% Triton X100 for 10 min. All samples were blocked with 5% bovine serum albumin (BSA)-PBS solution for 2 h at room temperature. Blocking buffer was discarded and samples were washed with PBS three times. Primary mouse anti-human vinculin antibodies (1:100 in 1% BSA-PBS solution; Sigma Aldrich, Oslo, Norway) were incubated with the samples overnight at 4°C. Samples were washed with PBS three times prior to 1 h incubation with Alexa Fluor 647 Phalloidin (1:400, ThermoFisher Scientific, Waltham, MA) and goat anti-mouse IgG secondary antibodies Alexa Fluor 488 (ThermoFisher Scientific). Secondary antibodies were discarded, and wells were washed with PBS three times. 4′,6-diamidino-2-phenylindole (DAPI) was used (1:1000, ThermoFisher Scientific) to stain the nuclei. Gels were viewed with a 20x/0.40 HCX PL APO CS objective lens on an upright confocal microscope (TCS SP8, Leica Microsystems, Wetzlar, Germany) using 638 nm excitation.

Cell activity and differentiation

The effect of soluble factors from different scaffolds on hMSC metabolism and differentiation was investigated indirectly in an exposure setup. In all, 3.0 x 10^4 cells were seeded on the base of tissue culture plates (24-well, Nunc, Roskilde, Denmark). Upon confluency, mineralised and non-mineralised hydrogel discs (20 μl, ⌀ ~5 mm, t ~1 mm) were placed in hanging inserts above the cultured cells (polycarbonate membranes, pore size 3 μm, Merck Millipore, Burlington, MA) for 2, 7, 14 and 21 days. Six independent replicates were cultured for each test and control setup.

Calcium and zinc concentration measurements. Calcium and zinc concentrations in the cell culture medium over time were determined by atomic absorption spectroscopy (AAS; AANALYST 400, Perkin Elmer, Waltham, MA). Lanthanum chloride was added to AAS samples at a concentration of 10 mg/mL to precipitate phosphate. Air/acetylene was used as carrier gas. Media from six individual replicates were collected. Two replicates per time point were pooled resulting in three samples from which data were collected (n = 3).

Cytotoxicity. Cytotoxicity was measured for cells indirectly exposed to hydrogel scaffolds for 72 h using a lactate dehydrogenase (LDH) detection kit (Roche, Basel, Switzerland). Cytotoxicity was determined by extracellular LDH activity upon media collection relative to positive and negative controls. Cells cultured on tissue culture polystyrene (TCPS) with and without 0.1% Triton X100 were used as a positive and negative controls, respectively. Absorbance values were determined at 490 nm (n = 6). Data are presented as a percentage of maximum cytotoxicity relative to the positive control.

Cell viability. Cell viability was assessed using an Alamar blue assay. After 72 h of indirect exposure, medium was replaced with fresh medium containing 10% Alamar blue solution (Thermo Fisher Scientific). Plates were protected from light and incubated for 4.5 h at 37°C. Alamar blue reduction was determined by reading fluorescence at 590 nm (530 nm excitation). Values were normalised to Alamar blue reduction of cells relative to controls (negative control, non-exposed cells on TCPS; positive control, Alamar blue reagent in cell culture medium completely reduced by autoclaving). Cell-free samples were tested to verify that scaffolds did not interfere with the assay.

Alkaline phosphatase activity. Alkaline phosphatase (ALP) activity was evaluated using a p-nitrophenol (pnPP; Sigma Aldrich) assay at 7 and 14 d. Medium from the wells was discarded and samples were washed with PBS twice. Cells were lysed by adding 500 µL deionised water. In addition, cells were scraped off the plate surface using a sterilised spatula. Lysed cells in deionised water were collected in test tubes and placed in a bath at 37°C for 1 h. The tubes were afterwards frozen at -80°C for 1 h. Before the ALP the assay, samples were allowed to defrost at room temperature and centrifuged. Samples (25 µL) were mixed with 75 µL pnPP. Plates were incubated protected from light at room temperature for 30 min before adding 50 µL of 3 M sodium hydroxide to stop the reaction. Absorbance was read at 405 nm. ALP activity was calculated using standards (calf intestinal ALP).

Multiplex immunoassay. Multianalyte profiling was performed to measure bone marker proteins in cell culture medium secreted from hMSCs at day 2, 7, 14 and 21 using the Luminex 200 system (Luminex, Austin, TX). Median fluorescent intensity was analysed using a 5-parameter logistic line-curve fitting method for calculating analyte concentrations in samples via the xPONENT 3.1 software (Luminex). Levels of interleukin-6 (IL-6), tumour necrosis factor alpha (TNFα), osteoprotegrin (OPG), osteopontin (OPN), osteocalcin (OC), and sclerostin (SOST) were measured using Human Bone Magnetic Bead Panel kit (EMD Millipore, Billerica, MA). The assay was performed according to the protocol provided by the manufacturer.

Reverse-transcriptase polymerase chain reaction (RT-PCR). The expression of bone-related genes, *runt-related transcription factor 2* (*RUNX2*), *osteopontin* (*OPN*), *osteocalcin* (*OC*) and *osterix* (*OSX*) were evaluated via RT-PCR. Stem cells exposed to non-mineralised and mineralised hydrogels were lysed after 14 and 21 days of exposure and total RNA was extracted using Trizol reagent (Invitrogen, USA) in accordance to the protocol provided by the manufacturer (n = 6 per group and time point). Total RNA was quantified using absorbance ratios of 260/280 and 260/230 nm measured on a NanoDrop One spectrophotometer (Thermo Fisher Scientific). In all, 1 µg of RNA was utilised for first-strand cDNA synthesis using a commercial kit (#K1612, Thermo Fisher Scientific). The RT-PCR reaction was performed using iQ™ SYBR® Green Supermix in a CFX™ Connect cycler (Bio-Rad, Hercules, CA) and the primers listed in Table 2. Data were analysed using the comparative CT method (ΔΔCt) method and normalised to glyceraldehyde-3-phosphate dehydrogenase (*GAPDH*) expression.

Table 2. List of primers used in this study.

Gene	Primer sequence
RUNX2	F: 5'TTACTTACACCCCGCCAGTC 3' R: 5'CACTCTGGCTTTGGGAAGAG 3'
OPN	F: 5'GCCGAGGTGATAGTGTGGTT 3' R: 5'TGAGGTGATGTCCTCGTCTG 3'
OC	F: 5'GCAAGTAGCGCCAATCTAGG 3' R: 5'GCTTCACCCTCGAAATGGTA 3'
OSX	F: 5'TACCCCATCTCCCTTGACTG 3' R: 5'GCTGCAAGCTCTCCATAACC 3'
GAPDH	F: 5'CTCTGCTCCTCCTGTTCGAC 3' R: 5'ACGACCAAATCCGTTGACTC 3'

Cell-mediated matrix formation

Scanning electron microscopy. Cell-mediated formation of mineralised matrix on different scaffolds was assessed by scanning electron microscopy (S-4800, Hitachi, Shibuya, Japan). In all, 7.5 x 10^3 hMSCs were seeded on scaffold discs as described in section 2.4 and cultured for 21 d (n = 2 per group). Samples were fixed with 4% PFA and washed twice with PBS followed by water replacement via ethanol series (10 min each in 50%, 80%, 90%, 95% and 100% ethanol). Consequently, ethanol was exchanged with hexamethyldisilazane and samples were air-dried. Prior to SEM imaging, dried samples were sputter coated with 10 nm platinum.

Alizarin red. The effect of soluble factors from different scaffolds on hMSC extracellular calcium deposition was investigated in an exposure setup as performed when assessing cell activity and differentiation. Four independent replicates were cultured for all experiments. Cells were cultured on the base of 24-well plates with exposure to the different scaffolds for 21 days. After fixation with 4% PFA, cells were washed with PBS. Cells were then incubated in alizarin red solution (2% w/v) for 5 min. The solution was discarded and cells were washed with distilled water, followed by optical microscopy using 5x and 10x objectives (Leica DM IL, Germany). In order to quantify alizarin red staining from each sample, cetyl pyridium chloride (10% w/v) was added to each well and incubated at room temperature for 30min. Absorbance was read at 562 nm.

Statistical analysis

Differences between groups were statistically assessed via analysis of variances using SigmaPlot 14.0 (Systat Software Inc., USA). Post hoc Dunnett's test was performed if groups were compared to controls, post hoc Tukey test was used for pairwise comparison between different groups. Normality was tested by a Shapiro-Wilk test. If the normality test was failed, one-way analysis of variance (ANOVA) on ranks (Kruskal–Wallis test) and post hoc Dunn's test was performed. For all tests, a value of $p < 0.05$ was considered significant. Data in all figures are presented as mean ± standard deviation.

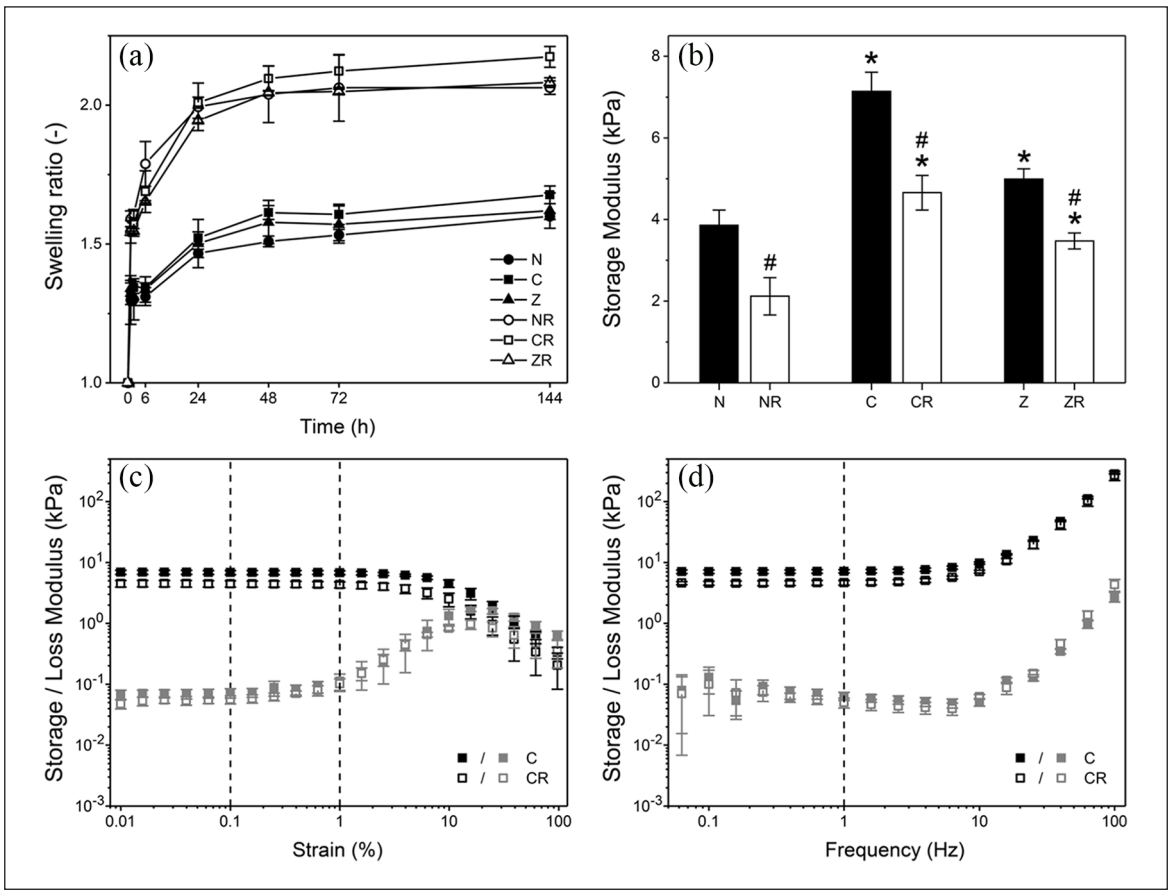

Figure 1. Mechanical characterisation of a non-mineralised hydrogel (N) and composites with citrate (C) or zinc (Z) depend on presence of mineral and cRGD-functionalisation (suffix R). (a) Volume swelling ratios versus time in cell culture medium. (b) Comparison of storage moduli of all sample groups as determined in oscillatory shear at 1 Hz and 0.1% strain. (c) Exemplary oscillatory shear strain sweeps of C composites with and without cRGD at 1 Hz frequency. (d) Exemplary frequency sweeps for the same samples at 0.1% strain.

Mean values and standard deviation are shown for all samples (n = 3). * indicates significance compared to non-mineralised scaffolds with same cRGD-functionalisation, # indicates significance compared to cRGD-free scaffolds ($p < 0.05$).

Results and discussion

Scaffold characterisation

Hydrogel elasticity has previously been identified as one of the key factors controlling stem cell attachment, organisation, and differentiation.[22,24] We therefore characterised swelling behaviour and mechanical properties of non-mineralised hydrogels, (N), citrate- (C), or zinc-stabilised composites (Z). Furthermore, the effect cRGD motifs on the physical scaffold properties was investigated. These motifs were tethered to the PEG-macromers to provide attachment sites for cells directly seeded onto the scaffolds.

In contact with cell culture medium, both non-mineralised and composite hydrogel scaffolds exhibited notable swelling (Figure 1(a)). Volumetric swelling measurements revealed that swelling persisted for 48 h in all tested materials. After this time point, no further statistically significant increase in volume was observed. Related to the polymer content, the observed swelling ratios were similar to those reported elsewhere.[25,26] Interestingly, no statistically significant differences were found comparing swelling of non-mineralised and mineralised scaffolds. This indicates that mineral particles in the composites did not considerably restrict polymer chain stretching. The incorporation of cRGD, on the other hand, resulted in approximately 30% higher equilibrium swelling ratios (~2.1) compared to scaffolds without cRGD (~1.6). This can be explained by the fact that cRGD motifs are tethered to the same functional groups on the polymer that are also used for end-linking. Functional groups that are occupied by cRGD are no longer able to form cross-links; a looser network with less elastically effective chains is formed. Interestingly, this observation stands in contrast to findings we earlier reported for similar hydrogels.[22] Investigating similar hydrogels, we found no significant effect of the presence of cRGD-functionalisation on the swelling ratio. It is important to notice that in our previous study hydrogels were formed with twice the polymer content as in the

present study. Consequently, in the present study, the same absolute amount of incorporated cRGD corresponds to a higher relative reduction in functional groups available for end-linking, which explains the increased impact of cRGD incorporation on swelling rations.

The mechanical properties of the different scaffolds after swelling were characterised by rheology. Exemplary amplitude and frequency sweeps for citrate-stabilised composites with and without cRGD-functionalisation are shown in Figure 1(c) and (d). All scaffolds exhibited elastic, solid-like behaviour for strains up to 1% and frequencies below 10 Hz. In the linear-elastic regime, storage moduli ranged from 2.1 to 7.1 kPa depending on the mineralisation and cRGD-functionalisation (Figure 1(b)). Incorporation of cRGD significantly affected the mechanical properties, which is consistent with the results from swelling measurements. Storage moduli were 30%–45% lower for cRGD-functionalised composites compared to non-functionalised ones. The reduction in storage modulus due to cRGD incorporation was most pronounced for non-mineralised hydrogels. Notably, the stiffness of non-mineralised scaffolds was considerably higher than the values reported for similar hydrogels based on four-armed macromers,[23,25,26] despite the lower initial polymer content. This indicates that in the present hydrogels a larger proportion of functional groups resulted in elastically effective cross-links, that is., less heterogeneous networks were formed.

Despite their similar swelling ratios, rheometry further showed that mineralised composites were significantly stiffer than non-mineralised hydrogels, as reported elsewhere.[27] This suggests that the presence of mineral in the scaffold increased the resistance to elastic deformation without affecting their network architecture. The mineral-induced stiffening effect was particularly prominent for citrate-stabilised composites, which featured 80% and 120% higher storage moduli than non-mineralised hydrogels in the absence and presence of cRGD, respectively. After 3 days of ageing in buffer, the CaP mineral in citrate-stabilised composites consists of a mix of OCP and HA crystals that exhibit an entangled plate-like morphology.[11] It appears intuitive that these entangled crystals contribute to the mechanical properties to a higher degree than the spherical ACP particles that we found in zinc-doped composites.

Cell attachment

PEG-based hydrogels are known for their low protein adsorption, which also makes them inherently non-adherent for cells. The ability of cells to adhere to the substrate not only dictates their morphology, but can also determine their capacity to differentiate towards a specific lineage.[28,29] Synthetic hydrogels have been rendered cell-adhesive upon incorporation of whole extracellular matrix (ECM) proteins or via bio-functionalisation with cRGD motifs.[22,30,31] Concurrently, there is evidence that minerals can serve as protein attachment sites, which raises the question if the presence of these minerals is sufficient to serve as anchoring sites for cell adhesion.[32] Figure 2 presents confocal microscopy images of mineralised and non-mineralised hydrogels with and without cRGD. Cells seeded on hydrogels in the presence of minerals exhibited morphologies similar to those on non-mineralised gels. In all confocal images of hMSCs on gels without cRGD (Figure 2(a)–(c)), cells appeared rounded and fewer in number compared to hydrogels functionalised with cRGD, where cells have more spread morphologies (Figure 2(d)-(f)). Irrespective of the presence of minerals, it is evident that cRGD is essential for cells to adhere in spread morphology on the surface of the investigated scaffolds.

Confocal microscopy further showed no peripheral localisation of vinculin, irrespective of the presence of minerals. This is similar to our findings previously reported on soft and stiff non-mineralised PEG hydrogels.[22] In addition, the absence of mature focal adhesions in cells cultured with osteogenic differentiation media has previously been attributed to a loosely adherent phenotype and lower cell motility, which was interpreted as a sign of induced osteogenesis.[33]

ECM formation of hMSCs seeded directly onto cRGD-functionalised scaffolds was qualitatively investigated by SEM. Cells on citrate- or zinc-stabilised composites formed significantly more heavily mineralised ECM compared to cells on non-mineralised scaffolds (Supplementary Figure S 1). This suggested that factors released from scaffolds with stabilised amorphous CaP might support osteogenic differentiation and matrix mineralisation facilitating bone formation.

Biocompatibility and cell differentiation

Cation release and cell viability. We used an exposure setup to investigate the effects of the observed release of calcium and zinc ions on matrix mineralisation, hMSC activity, and differentiation. Scaffolds were formed under mildly acidic conditions to mimic gelation in inflammatory environments, where pH values as low as 3.7 have been detected.[34] The low reaction pH, however, entails a relatively high solubility of CaPs during composite formation. This means that a substantial fraction of ions remains unprecipitated within the scaffolds. When immersed in cell culture medium, these ions readily diffuse out of the hydrogel matrix. After this initial release, more ions are released when mineral particles dissolve, as expected for low crystalline phases.[11]

Calcium and zinc concentrations in the cell culture medium over time in the presence of the different scaffolds are shown in Figure 3(a) and (b). For non-mineralised hydrogels, calcium concentrations of roughly 80 mg/L were measured steadily throughout the experiment.

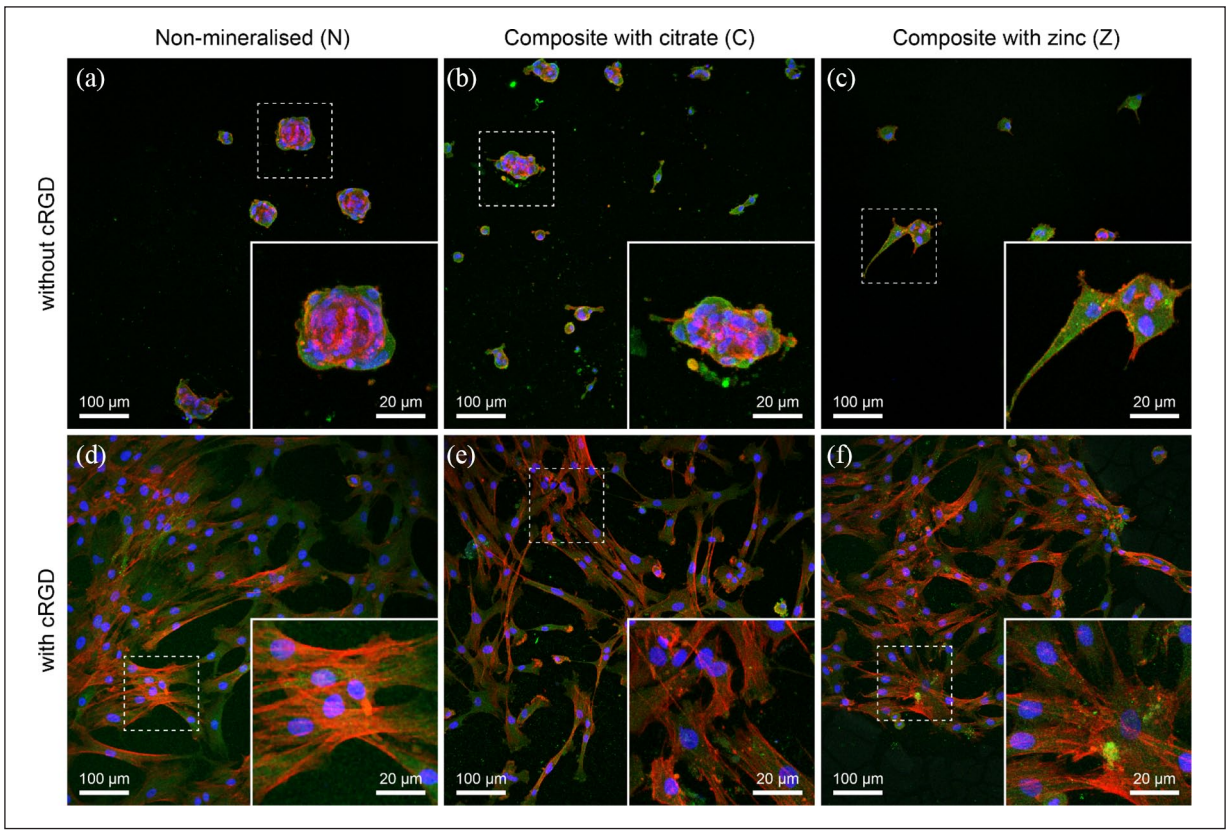

Figure 2. Confocal images of hMSCs on hydrogels and composites with and without 2.5 mM of cRGD. hMSCs were immunolabelled for actin (red), vinculin (green) and DAPI (blue). (a-c) Representative images show cells seeded on non-mineralised (N) and composite hydrogels (C and Z) indicating the lack of spreading of hMSCs in the absence of cRGD. (d-f) Alternatively, images represent cells adopting a spread morphology when cultured on non-mineralised or composite hydrogels in the presence of cRGD tethered to the hydrogels.

The only calcium source present in this group was the cell culture medium itself. In the presence of zinc- and citrate-containing composites, calcium concentrations were approximately three- and twofold higher, respectively, compared to non-mineralised hydrogels at the first medium change (Figure 3(a)). From the second medium change onwards, medium calcium concentrations in the presence of zinc-doped composites were similar to those of the plain cell culture medium. For citrate-stabilised composites, however, medium calcium concentrations were significantly lower than those measured in medium alone. Observations of citrate-stabilised composites indicated the initial mineral particles in the hydrogel matrix gradually dissolve over the course of days (Supplementary Figure S 2).[11] Initially, the reduced medium calcium concentration in the presence of citrate-stabilised composites might be partially attributed to chelation of free calcium by released citrate. With each medium change, however, the citrate concentration in the medium would be further decreased suggesting that the medium calcium concentration should approach that of plain medium over time. Meanwhile, we observed significant mineral deposition in the cell sheets in the presence of mineralised composites (Figure 4(a)–(c)). This leads us to believe that the low medium calcium concentrations are a consequence of more calcium being consumed in ongoing mineral precipitation in the ECM of the cell sheets, which is facilitated by ECM proteins such as collagen, than is supplied by the dissolution of citrate-stabilised mineral particles in the scaffolds.

Zinc concentrations in the medium were constantly below 1 mg/L (the normal serum level in humans)[35] for both non-mineralised hydrogels and citrate-stabilised composites. In the presence of zinc-doped composites, we found a high initial zinc release resulting in a concentration around 22 mg/L followed by a sustained release with concentrations slowly decreasing from 7 to 4 mg/L. The initial release can again be interpreted as a result of the high concentration of unprecipitated ions in the freshly formed composites. The sustained release indicates that zinc-doped ACP was slowly dissolving, which is in agreement with earlier observations.[11] Interestingly, at later time points, the zinc concentration in medium was close to 3 mg/L, which has previously been shown to induce a significant increase in osteogenic differentiation and mineralisation in hMSCs.[36]

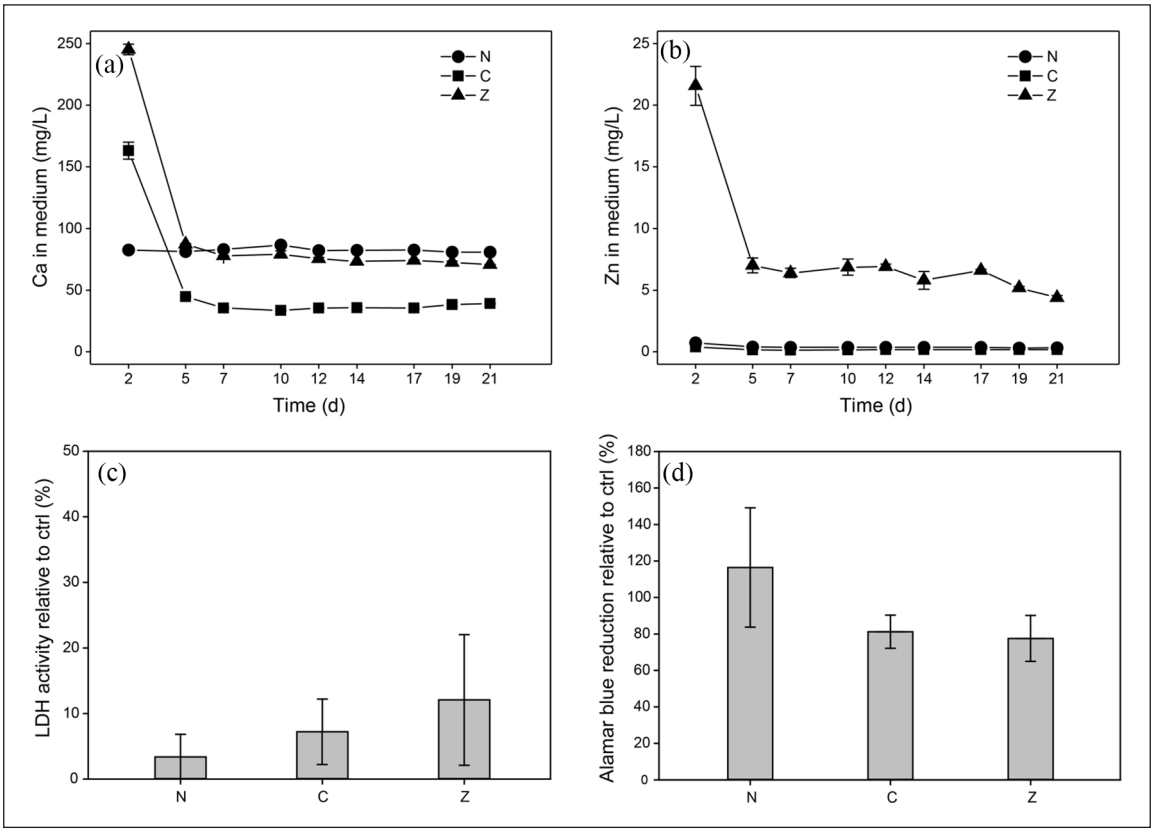

Figure 3. (a, b) Calcium and zinc concentrations in cell culture media exhibit an initial burst release followed by steady concentration levels over time for both citrate- (C), and zinc-stabilised composites (Z). Calcium and zinc levels for non-mineralised hydrogels (N) correspond to the concentrations of the cell culture medium. Where error bars are not visible, standard deviations are smaller than symbols. Assessment of membrane integrity and cell metabolism of hMSCs after 72 h of exposure indicated no negative effects of mineralised and non-mineralised hydrogel scaffolds compared to TCPS controls. **(c)** Membrane integrity determined via extracellular LDH activity relative to controls (negative control, non-exposed cells on TCPS; positive control, cells lysed with Triton X-100). (d) Alamar blue reduction as a measure of cell metabolism relative to controls (negative control, non-exposed cells on TCPS; positive control, Alamar blue reagent in cell culture medium completely reduced by autoclaving). Graphs show mean values and standard deviations (n = 6).

As we introduced cells to an environment with potentially cytotoxic ion concentrations, we assessed cell membrane integrity via LDH assay.[37] Our results indicated no significant cytotoxic effects for hMSCs exposed to any of the scaffolds (Figure 3(c)). In addition, cell viability was assessed via Alamar blue assay, which indicated that cells exposed to non-mineralised gels exhibited slightly higher viability and metabolic activity compared to those exposed to mineralised hydrogels (Figure 3(d)). However, the observed differences were not statistically significant.

ECM mineralisation and osteogenic cell differentiation. Appearance and ECM mineralisation of the cell sheets was investigated by phase contrast microscopy and alizarin red staining (Figure 4(a)-(c)). Images acquired one day prior to the LDH and Alamar blue assays revealed notable qualitative differences among the groups. In cell sheets exposed to citrate- and zinc-stabilised hydrogels, scattered clusters of mineral particles were observed, which persisted until day 21 (arrowheads in Supplementary Figure S 3). No mineral clusters were seen for cells exposed to non-mineralised scaffolds, which formed a uniform, confluent monolayer. Notably, in the presence of citrate- or zinc-stabilised composites, the cell sheets did not cover the entire TCPS surface and exhibited fluctuations in cell density (dashed ellipses in Figure 4(a)), which could explain the lowered metabolic activity observed in the Alamar blue assay (Figure 3(d)).

Alizarin red staining confirmed the systematic differences in calcium deposition within cell sheets exposed to the different scaffolds. Optical microscopy images of alizarin red stained cell sheets clearly indicate an abundance of calcium deposits in the ECM of cells exposed to mineralised scaffolds (Figure 4(b)). Quantitative analysis of alizarin red staining confirmed a significant increase of ECM mineralisation in the presence of both citrate- and zinc-containing mineralised hydrogels compared to non-mineralised hydrogels (Figure 4(c)). For non-mineralised hydrogels, no calcium deposition was observed in the absence of cells,

whereas some calcium deposition occurred in the presence of hMSCs. This is likely a consequence of the presence of osteogenic supplements in the cell culture medium and increased cell-to-cell contact driving differentiation and matrix production.

Conversely to the significant differences in ECM mineralisation, membrane-bound ALP activity measured after 7 and 14 days of exposure to the different scaffolds did not reveal any significant differences in osteogenic differentiation (Figure 4(d)). For all groups, ALP activity was significantly higher after 14 versus 7 days of exposure. The high ALP activity at day 14 suggests that hMSCs were no longer in an undifferentiated state and implies commitment towards the osteogenic lineage.[38] It is surprising, however, that ALP activity was not significantly increased by the presence of zinc, as this stands in contrast to observations made *in vitro* and *in vivo*.[39,40] On the contrary, one study in particular cultured rat bone marrow stromal cells supplemented with soluble zinc and reported no significant increase in ALP activity with the presence of zinc.[41]

To further evaluate the commitment of hMSCs to the osteogenic lineage, we investigated the presence of osteogenic proteins secreted by the cells and the expression of osteogenic genes on RNA level. Proteins secreted by hMSCs were analysed using a multiplex immunoassay after 2, 7, 14, and 21 days of exposure to non-mineralised and composite hydrogels. Generally, IL-6 and TNFα levels were not significantly different for composite hydrogels compared to non-mineralised controls (Figure 5(a) and (b)). However, zinc-stabilised composite hydrogels exhibited significantly higher levels of IL-6 compared to the non-mineralised controls and higher amounts of TNFα compared to the other groups at all time points but specifically at day 2. This increase may likely be a consequence of the cells being initially exposed to elevated zinc concentrations (Figure 3(b)).[42]

Analysis of osteogenic proteins secreted by hMSCs at different time points can provide insights into the differentiation patterns adopted by stem cells in inductive environments (Figure 5(c)–(f)).[38] In particular, protein secretion of OC, OPN, and SOST were highest at day 21 for most groups, confirming that cells had committed to osteogenic differentiation. In addition, OPG expression was highest at day 14, irrespective of the scaffold type. Overall, no prominent stimulating effects exclusive to composite scaffolds were observed. Though this was unexpected, there are several possible explanations for this observation. For all groups, hMSCs were cultured in media containing osteogenic supplements. This implies that potential osteogenic effects imposed by the presence of soluble minerals may have been masked by the stimulatory effects of the osteogenic supplements in the medium itself. The fact that the protein expression for all groups followed similar trends indicates that the driving force in the differentiation of hMSCs appeared to be largely influenced by the presence of osteogenic supplements rather than ions released by the composites. As a

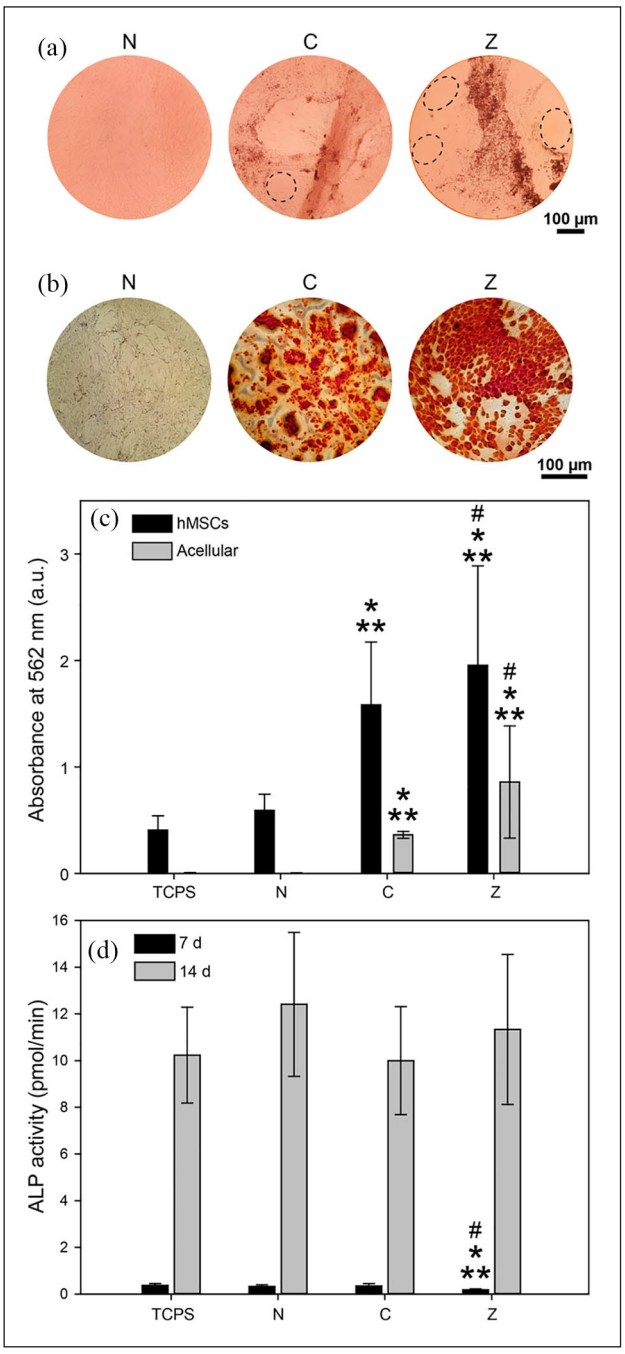

Figure 4. (a) Phase contrast microscopy images reveal differences in cell sheet mineralisation of hMSCs after 21 d of exposure to non-mineralised (N), citrate- (C), and zinc-stabilised composites (Z). In addition, cell coverage varied considerably across the different groups (dashed ellipses indicate areas not covered by cells). **(b)** Alizarin red staining revealed increased ECM mineralisation for cells exposed to mineral-containing composites. **(c)** Quantification of alizarin red assay based on absorbance values at 562 nm (n = 4). (d) Membrane-bound ALP activity of hMSCs increased significantly between day 7 and 14 of exposure, indicating osteogenic differentiation irrespective of the scaffold group (n = 6). Bars represent mean values and standard deviation, **indicates statistical significance compared to TCPS control (cells not exposed to scaffold), *compared to N, and # compared to C ($p < 0.05$).

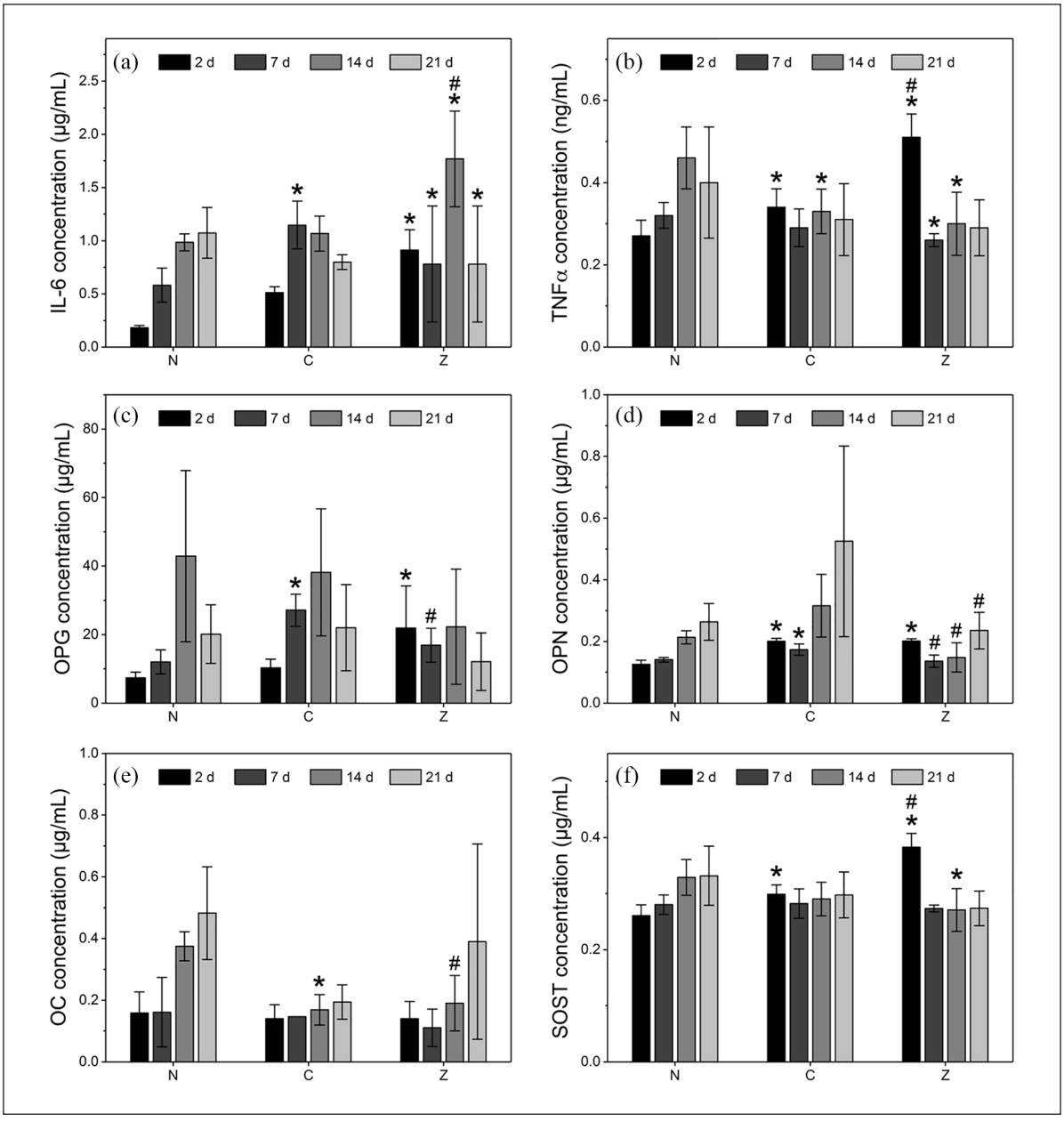

Figure 5. Cytokines and proteins measured from medium of hMSCs exposed to non-mineralised hydrogels (N), citrate- (C), and zinc-stabilised composites (Z). (a) Inflammation markers interleukin-6 (IL6) and (b) tumour necrosis factor α (TNFα) are shown among bone markers (c) osteoprotegerin (OPG), (d) osteopontin (OPN), (e) osteocalcin (OC), and (f) sclerostin (SOST). Osteogenic proteins such as OPG, OPN and OC are highest at day 14 or 21, indicating that cells are transitioning towards the osteogenic lineage. However, despite the initial release of calcium of zinc, no significant differences among the groups are observed at early timepoints.

Bars represent mean values and standard deviations (n = 6). * indicates statistical significance compared to N, # compared to C (both $p < 0.05$).

result, no noticeable effects on the osteogenic differentiation of hMSCs could be observed for the composite scaffolds. Various studies have investigated whether the influence of osteogenic additives as part of the cell culture media is responsible for the differentiation of cells within treatment groups for a range of scaffolds.[43–45] For instance, Müller and colleagues[43] observed increased ALP activity and expression of osteogenic genes in cells cultured on calcium phosphate surfaces in the absence of osteogenic additives. However, their results were largely attributed to physical cell-matrix interactions rather than the presence of dissolved ions.

In addition to analysing the protein secretome of hMSCS, gene expression for both early and late osteogenic differentiation markers *RUNX2, OC, OPN* and *OSX* was

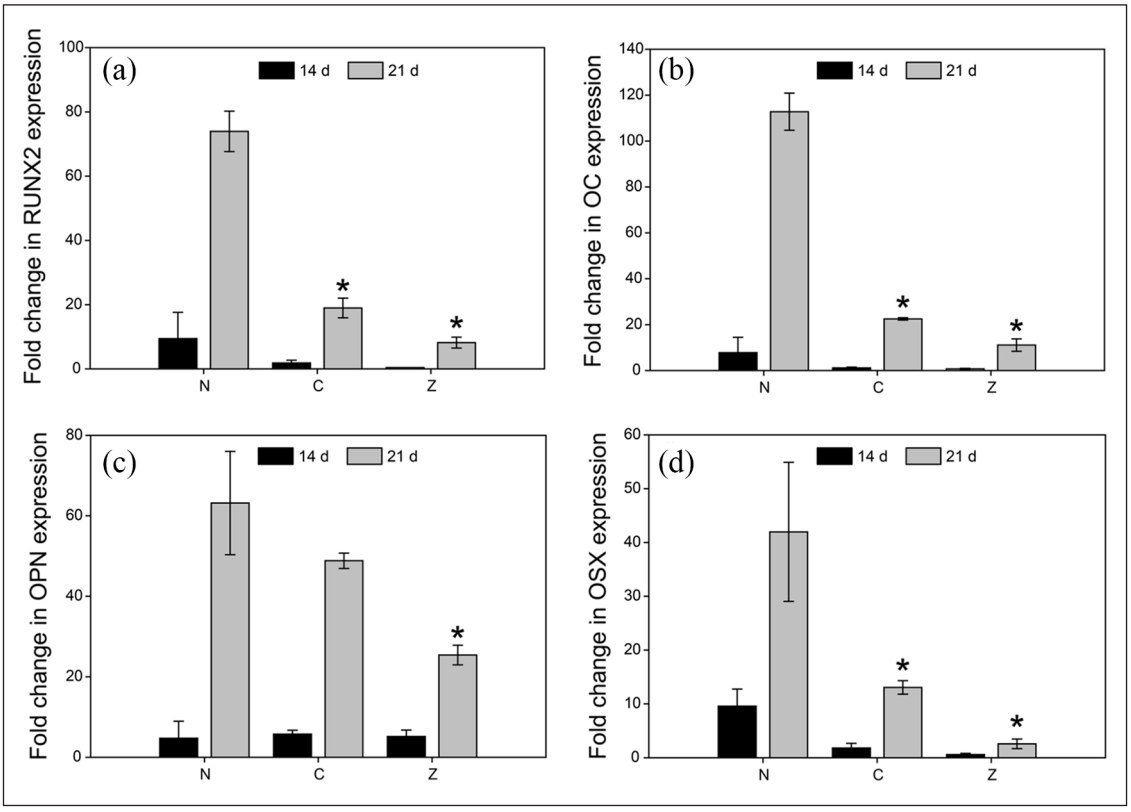

Figure 6. RT-PCR of genes involved in osteogenic differentiation of hMSCs show a significant increase in gene expression between 14 and 21 d for (a) Runt-related transcription factor 2 (*RUNX2*), (b) Osteocalcin (*OC*), (c) Osteopontin (*OPN*), and (d) Osterix (*OSX*). Cells were cultured in the presence of non-mineralised hydrogels (N), citrate- (C), and zinc-stabilised composites (Z). Data is presented as fold-changes normalised to the housekeeping gene expression (GAPDH) levels. Bars represent the mean and standard deviation (n = 6), * indicates statistical significance compared to N.

assessed (Figure 6). Irrespective of exposure to any scaffold group, all genes exhibited significantly higher fold changes at 21 d versus 14 d. However, gene expression at 21 d was highest for cells exposed to non-mineralised hydrogels for all genes analysed. One explanation could pertain to the depletion of zinc available to the cells over time. As shown in the release studies, the zinc concentration in the culture media changed from initially 22 mg/L to a sustained level of approximately 7–4 mg/L after 5 days (Figure 3(b)). Other studies that show an upregulation of osteogenic genes such as *RUNX2* in the presence of zinc tend to replenished cell culture media with zinc every 2 days to maintain high concentrations of the metal available to the cells.[46] However, irrespective of the availability of zinc, one would expect the changes in gene expression to be at least at par with that of the control group lacking mineral supplementation altogether. While zinc-stabilised composites exhibited a controlled release of zinc (Figure 3(b)), higher concentrations over longer periods of time may be required to drive osteogenic gene expression. It was to our surprise that *RUNX2* and *OSX* expression in particular were not upregulated in the presence of zinc, since zinc itself is known to synergistically mediate osteogenic differentiation via these genes.[47] However, zinc is likely to interact and precipitate with anions or bind to serum albumin present in the cell culture medium, thereby reducing the concentration of free zinc ions available to the cells.

Comparing gene expression levels between cells exposed to citrate- and the zinc-stabilised composites, in all instances cells exposed to citrate-stabilised composites showed higher fold changes compared to zinc-stabilised composites. Nevertheless, statistical analysis found the differences in gene expression between citrate- and zinc-stabilised composites to be insignificant. Finally, as observed in the protein secretion of OPN and OC (Figure 5(c) and (e)), the expression of these genes was highest at day 21 for all groups. This implies that the cells have terminally differentiated towards the osteogenic lineage, irrespective of the presence of ACPs. We observed mineral precipitation within the ECM of the cell sheets as seen in Figure 4(b) and Supplementary Figure S1. Along with the low concentrations of calcium and zinc ions in the cell culture media, this suggests that after the initial burst release, cells are exposed to reduced amounts of zinc and calcium ions, likely explaining why we see a reduction in gene expression levels for the cells exposed to the composite hydrogels.

Conclusion

The aim of this study was to investigate the attachment of hMSCs on hydrogel-ACP composites and the osteogenic effect of soluble factors from these scaffolds. Physical characterisation showed that the formed scaffolds featured improved mechanical properties compared to similar PEG-based matrices. Stiffness was significantly increased in the presence of CaP mineral. The two-dimensional attachment setup showed that the presence of CaP mineral alone was insufficient for cell attachment and cRGD functionalisation of the hydrogel was required to promote cell attachment of large numbers of cells with spread morphology. Protein and cytokine analysis suggested that the high initial zinc release from zinc-doped composites provoked a mild inflammatory response in primary human hMSCs. However, cell membrane integrity and viability assays showed that all tested scaffolds were cytocompatible.

Cell sheets exposed to citrate-and zinc-stabilised composites showed significantly increased mineralisation and increased levels of osteogenic proteins compared to non-mineralised scaffolds up to 1 week of exposure. At later time points, however, both osteogenic protein levels and expression of osteogenic genes were found to be reduced in the presence of mineralised composites. While more research is needed to exclude potential masking effects from osteogenic supplements in the cell culture medium, the observations suggest that soluble factors released from composites containing stabilised amorphous CaP mineral are effective at stimulating early ECM mineralisation and osteogenic differentiation. This makes the evaluated composite scaffolds interesting for applications in non-healing bone defects. Particularly, zinc-stabilised composites could be a promising system for their capacity to facilitate a tailored release of zinc ions acting as a bioinorganic drug.

Declaration of conflicting interests

The author(s) declared no potential conflicts of interest with respect to the research, authorship, and/or publication of this article.

Funding

The author(s) disclosed receipt of the following financial support for the research, authorship, and/or publication of this article: This work was supported by the Osteology Foundation (grant number 15-091) and the Research Council of Norway (FRINATEK grant number 231530). The authors would sincerely like to thank Manuel Gómez-Florit and Mousumi Sukul for their help with the Alizarin red and RT-PCR experiments.

ORCID iDs

Håvard J Haugen https://orcid.org/0000-0002-6690-7233
Hanna Tiainen https://orcid.org/0000-0003-2757-6213

Supplemental material

Supplemental material for this article is available online.

References

1. Giannoudis PV, Dinopoulos H and Tsiridis E. Bone substitutes: an update. *Injury* 2005; 36(Suppl. 3): 20–27.
2. Laurencin CT and El-Amin SF. Xenotransplantation in orthopaedic surgery. *J Am Acad Orthop Surg* 2008; 16(1): 4–8.
3. Arrington ED, Smith WJ, Chambers HG, et al. Complications of iliac crest bone graft harvesting. *Clin Orthop Relat Res* 1996; 329: 300–309.
4. Palmer SH, Gibbons CL and Athanasou NA. The pathology of bone allograft. *J Bone Jt Surg Brit* 1999; 81: 333–335.
5. Tomford WW. Transmission of disease through transplantation of musculoskeletal allografts. *J Bone Joint Surg Am* 1995; 77(11): 1742–1754.
6. Roberts TT and Rosenbaum AJ. Bone grafts, bone substitutes and orthobiologics: the bridge between basic science and clinical advancements in fracture healing. *Organogenesis* 2012; 8(4): 114–124.
7. Stevens MM. Biomaterials for bone tissue engineering. *Mater Today* 2008; 11: 18–25.
8. LeGeros RZ. Properties of osteoconductive biomaterials: calcium phosphates. *Clin Orthop Relat Res* 2002; 395: 81–98.
9. Lutolf MP and Hubbell JA. Synthetic biomaterials as instructive extracellular microenvironments for morphogenesis in tissue engineering. *Nat Biotechnol* 2005; 23(1): 47–55.
10. Lutolf MP, Weber FE, Schmoekel HG, et al. Repair of bone defects using synthetic mimetics of collagenous extracellular matrices. *Nat Biotechnol* 2003; 21(5): 513–518.
11. Schweikle M, Bjornoy SH, van Helvoort ATJ, et al. Stabilisation of amorphous calcium phosphate in polyethylene glycol hydrogels. *Acta Biomater* 2019; 90: 132–145.
12. Han Y, You X, Xing W, et al. Paracrine and endocrine actions of bone – the functions of secretory proteins from osteoblasts, osteocytes, and osteoclasts. *Bone Res* 2018; 6: 16.
13. Kawamura H, Ito A, Miyakawa S, et al. Stimulatory effect of zinc-releasing calcium phosphate implant on bone formation in rabbit femora. *J Biomed Mater Res* 2000; 50(2): 184–190.
14. Seo HJ, Cho YE, Kim T, et al. Zinc may increase bone formation through stimulating cell proliferation, alkaline phosphatase activity and collagen synthesis in osteoblastic MC3T3-E1 cells. *Nutr Res Pract* 2010; 4(5): 356–361.
15. Jung G-Y, Park Y-J and Han JS. Effects of HA released calcium ion on osteoblast differentiation. *J Mater Sci Mater Med* 2010; 21(5): 1649–1654.
16. Barradas AMC, Fernandes HAM, Groen N, et al. A calcium-induced signaling cascade leading to osteogenic differentiation of human bone marrow-derived mesenchymal stromal cells. *Biomaterials* 2012; 33(11): 3205–3215.
17. Sarem M, Heizmann M, Barbero A, et al. Hyperstimulation of CaSR in human MSCs by biomimetic apatite inhibits endochondral ossification via temporal down-regulation of PTH1R. *Proc Natl Acad Sci U S A* 2018; 115(27): E6135–E6144.

18. Ikeuchi M, Ito A, Dohi Y, et al. Osteogenic differentiation of cultured rat and human bone marrow cells on the surface of zinc-releasing calcium phosphate ceramics. *J Biomed Mater Res A* 2003; 67(4): 1115–1122.
19. Yamada Y, Ito A, Kojima H, et al. Inhibitory effect of Zn2+ in zinc-containing β-tricalcium phosphate on resorbing activity of mature osteoclasts. *J Biomed Mater Res A* 2008; 84A: 344–352.
20. Kawamura H, Ito A, Muramatsu T, et al. Long-term implantation of zinc-releasing calcium phosphate ceramics in rabbit femora. *J Biomed Mater Res A* 2003; 65(4): 468–474.
21. Patterson J and Hubbell JA. Enhanced proteolytic degradation of molecularly engineered PEG hydrogels in response to MMP-1 and MMP-2. *Biomaterials* 2010; 31(30): 7836–7845.
22. Chahal AS, Schweikle M, Heyward CA, et al. Attachment and spatial organisation of human mesenchymal stem cells on poly(ethylene glycol) hydrogels. *J Mech Behav Biomed Mater* 2018; 84: 46–53.
23. Schweikle M, Zinn T, Lund R, et al. Injectable synthetic hydrogel for bone regeneration: physicochemical characterisation of a high and a low pH gelling system. *Mater Sci Eng C Mater Biol Appl* 2018; 90: 67–76.
24. Engler AJ, Sen S, Sweeney HL, et al. Matrix elasticity directs stem cell lineage specification. *Cell* 2006; 126(4): 677–689.
25. Phelps EA, Enemchukwu NO, Fiore VF, et al. Maleimide cross-linked bioactive PEG hydrogel exhibits improved reaction kinetics and cross-linking for cell encapsulation and in situ delivery. *Adv Mater* 2012; 24(1): 64–702.
26. Lutolf MP and Hubbell JA. Synthesis and physicochemical characterization of end-linked poly(ethylene glycol)-co-peptide hydrogels formed by Michael-type addition. *Biomacromolecules* 2003; 4(3): 713–722.
27. Patel M, Betz MW, Geibel E, et al. Cyclic acetal hydroxyapatite nanocomposites for orbital bone regeneration. *Tissue Eng Part A* 2010; 16(1): 55–65.
28. Trappmann B, Gautrot JE, Connelly JT, et al. Extracellular-matrix tethering regulates stem-cell fate. *Nat Mater* 2012; 11(7): 642–649.
29. Lee J-H and Kim HW. Emerging properties of hydrogels in tissue engineering. *J Tissue Eng* 2018; 9: PMC5881958.
30. Herrick WG, Nguyen TV, Sleiman M, et al. PEG-phosphorylcholine hydrogels as tunable and versatile platforms for mechanobiology. *Biomacromolecules* 2013; 14(7): 2294–2304.
31. Groll J, Fiedler J, Engelhard E, et al. A novel star PEG–derived surface coating for specific cell adhesion. *J Biomed Mater Res A* 2005; 74(4): 607–617.
32. Oliveira AL, Alves CM and Reis RL. Cell adhesion and proliferation on biomimetic calcium-phosphate coatings produced by a sodium silicate gel methodology. *J Mater Sci Mater Med* 2002; 13(12): 1181–1188.
33. Salasznyk RM, Williams WA, Boskey A, et al. Adhesion to vitronectin and collagen i promotes osteogenic differentiation of human mesenchymal stem cells. *J Biomed Biotechnol* 2004; 2004(1): 24–34.
34. Silver IA, Murrills RJ and Etherington DJ. Microelectrode studies on the acid microenvironment beneath adherent macrophages and osteoclasts. *Exp Cell Res* 1988; 175(2): 266–276.
35. Underwood EJ. 8 – Zinc. In: Underwood EJ (ed.) *Trace elements in human and animal nutrition*. 4th ed. Cambridge, MA: Academic Press, 1977, pp. 196–242.
36. Oh SA, Kim SH, Won JE, et al. Effects on growth and osteogenic differentiation of mesenchymal stem cells by the zinc-added sol-gel bioactive glass granules. *J Tissue Eng* 2011; 2010: 475260.
37. Koh JY and Choi DW. Quantitative determination of glutamate mediated cortical neuronal injury in cell culture by lactate dehydrogenase efflux assay. *J Neurosci Methods* 1987; 20(1): 83–90.
38. Stein GS, Lian JB, Stein JL, et al. Transcriptional control of osteoblast growth and differentiation. *Physiol Rev* 1996; 76(2): 593–629.
39. Yu J, Xu L, Li K, et al. Zinc-modified calcium silicate coatings promote osteogenic differentiation through TGF-β/Smad pathway and osseointegration in osteopenic rabbits. *Sci Rep* 2017; 7: 3440.
40. Luo X, Barbieri D, Davison N, et al. Zinc in calcium phosphate mediates bone induction: in vitro and in vivo model. *Acta Biomater* 2014; 10(1): 477–485.
41. Popp JR, Love BJ and Goldstein AS. Effect of soluble zinc on differentiation of osteoprogenitor cells. *J Biomed Mater Res A* 2007; 81(3): 766–769.
42. Bonaventura P, Lamboux A, Albarede F, et al. A Feedback Loop between Inflammation and Zn Uptake. *PLoS ONE* 2016; 11(2): e0147146.
43. Muller P, Bulnheim U, Diener A, et al. Calcium phosphate surfaces promote osteogenic differentiation of mesenchymal stem cells. *J Cell Mol Med* 2008; 12(1): 281–291.
44. Thibault RA, Scott Baggett L, Mikos AG, et al. Osteogenic differentiation of mesenchymal stem cells on pregenerated extracellular matrix scaffolds in the absence of osteogenic cell culture supplements. *Tissue Eng Part A* 2010; 16(2): 431–440.
45. Song SJ, Jeon O, Yang HS, et al. Effects of culture conditions on osteogenic differentiation in human mesenchymal stem cells. *J Microbiol Biotechnol* 2007; 17(7): 1113–1119.
46. Park KH, Choi Y, Yoon DS, et al. Zinc promotes osteoblast differentiation in human mesenchymal stem cells via activation of the cAMP-PKA-CREB signaling pathway. *Stem Cells Dev* 2018; 27(16): 1125–1135.
47. Fu X, Li Y, Huang T, et al. Runx2/osterix and zinc uptake synergize to orchestrate osteogenic differentiation and citrate containing bone apatite formation. *Adv Sci* 2018; 5(4): 1700755.